PHYSICAL REVIEW B VOLUME 23, NUMBER 2 15 JANUARY 1981

Site-selective excitation, crystal-field analysis, and energy transfer in europium-doped monoclinic gadolinium sesquioxide. A test of the electrostatic model

J. Dexpert-Ghys, M. Faucher, and P. Caro

Eléments de Transition dans les Solides, E.R. 060210 Centre National de la Recherche Scientifique, 1 Place A. Briand, 92190 Meudon, France

(Received 18 June 1980)

The fluorescence spectrum of Eu^{3+} in monoclinic Gd_2O_3 is analyzed at 300, 77, and 4.2 K. There are three distinct C_s crystallographic sites for the rare earth in the monoclinic structure. Through selective excitation of the three $^5D_0$ levels with a dye laser and time-resolution equipment, three different fluorescence spectra are obtained. To assign the spectra to definite crystallographic sites an electrostatic calculation of crystal-field parameters is undertaken for each site using the latest available structural data. The calculation involves both contributions from point charges and induced dipoles. The result is corrected for the shielding effect of 5*s* and 5*p* electrons and corrections to free-ion radial integrals are derived from experimental determination for other lanthanides in solids. Good agreement is found between simulated and experimental spectra, which allows an assignment of each of the three spectra to each of the three sites. Energy transfer from site to site is measured but is not interpreted at the moment.

I. INTRODUCTION

The absorption and fluorescence properties of Eu^{3+} in monoclinic Gd_2O_3 were first investigated by Rice and de Shazer.[1] They expected that the information could help to elucidate the nonradiative relaxation processes in oxides. They concluded that the Eu^{3+} ion occupies three nonequivalent sites of C_s symmetry but could not assign the spectral lines to any particular ion site. The aim of the present study is to complete and develop preliminary results[2] concerning selective site excitation in this material. The subject is in three parts:

The identification of the three distinct fluorescence spectra originating from $^5D_0$ levels of Eu^{3+} in the three crystallographic sites. This is done by using dye-laser selective site excitation of Eu^{3+}.

The assignment of each spectrum to Eu^{3+} in a definite crystallographic site. This is made possible by comparing experimental results and *a priori* calculations using the electrostatic model (point-charge and dipolar contributions).

Some comments about fluorescence rise and decay times and site-to-site energy-transfer properties.

II. CRYSTALLOGRAPHIC DATA

The monoclinic structure of rare earth sesquioxides is related to the hexagonal form and to the fluorite cell. In hexagonal Ln_2O_3 the Ln^{3+} ion is surrounded by six oxygens forming an octahedron, and a seventh along a threefold axis, the point symmetry being C_{3v}. The monoclinic structure was established for Sm_2O_3, Tb_2O_3, and Eu_2O_3 (see Refs. 3, 4, and 5). There are three nonequivalent point sites for Ln^{3+}, each of them of C_s symmetry. Following Cromer[3] the coordination around Ln III atoms can be described as a distorted octahedron with a seventh oxygen atom along a "threefold" axis, but at a very long distance (3.13 Å for Eu_2O_3). Ln I and Ln II have a sevenfold coordination with six oxygens at the apices of a trigonal prism and a seventh lying along the normal to a face. The positional parameters reported in Ref. 5 for Eu_2O_3 are probably very close to those of Gd_2O_3.

III. SAMPLE PREPARATION

Sintered samples were obtained by physical mixture of the oxides (95 at. % Gd_2O_3–5 at. % Eu_2O_3), pressed into thin plates, and fired in a lime-stabilized zirconia heating element at 1800 °C for 24 hours in an oxidizing atmosphere. The measured unit-cell parameters $a = 10.06$ Å, $b = 3.57$ Å, $c = 8.76$ Å, $\beta = 100°$ were those of pure monoclinic Gd_2O_3.

IV. EXPERIMENTAL

All the fluorescence spectra were recorded with a Jarrel-Ash 78460 Czerny-Turner spectrometer (focal length 1 m) at 300 K, 77 K or 4.2 K. Conventional ultraviolet excitation of Eu^{3+} was achieved by an Osram HBO 150-W lamp equipped with a Wood filter. Continous excitation of the Eu^{3+} $^5D_0$ level was accomplished by a Spectra Physics 375/376 cw single-mode jet-stream rhodamine 6*G* dye laser ($1\times10^{-3}M$ in ethylene glycol) pumped by a Spectra Physics 164 argon-ion laser. The wavelength of the laser beam was continuously tunable from about 5700 to 6500 Å, the linewidth being 0.7 cm^{-1}.

Pulsed excitation was obtained with the same assembly, the laser beam being chopped by an acousto-optic modulator (Soro *IM* 20) (Fig. 1). A boxcar integrator (ATNE) provides electronically gated signal processing and simultaneously

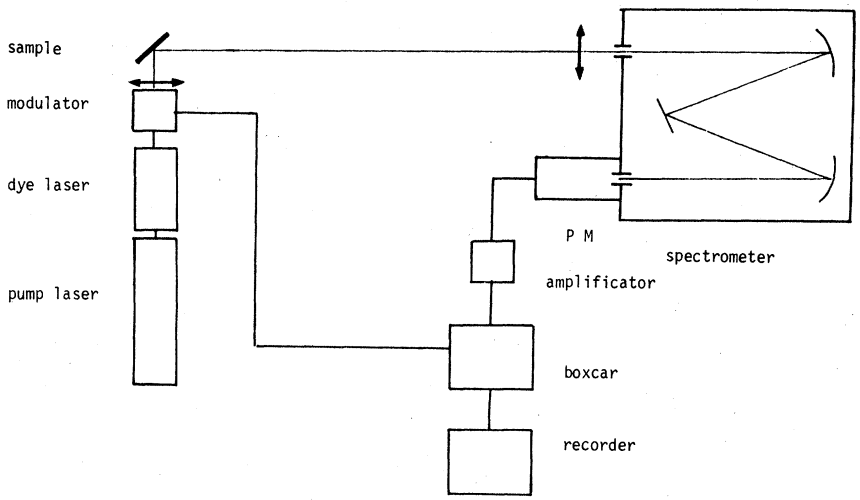

FIG. 1. Experimental apparatus.

triggers the modulator. The usual pulse duration was 30 μs. With the theoretical output power of 600 mW, a pulse corresponds to an 18-μJ energy and consequently to about 5×10^{13} photons. Time-resolved fluorescence spectra were obtained by analyzing each wavelength after a constant delay from the pulse start. Fluorescence-decay curves were recorded for a given wavelength by scanning the delay time between the pulse and the signal detection.

V. RESULTS. IDENTIFICATION OF *A,B,C,* SPECTRA

A. Steady-state fluorescence

The Eu^{3+} $^5D_0 \rightleftharpoons {}^7F_0$ transition wavelength falls in the broad emission range of the powerful Rh6*G* dye. The experiment consisted of exciting the Eu^{3+} $^5D_0$ level for a given crystallographic site and recording the corresponding $^5D_0 \rightarrow {}^7F_{1,2,3,4}$ fluorescence transitions.

Three lines were previously identified as $^5D_0 \rightarrow {}^7F_0$ transitions in Ref. 1 and the laser wavelength was tuned successively in exact resonance with each of them. Three distinct fluorescence spectra were thus obtained for the $^5D_0$ at 5786 Å (*A*), 5822 Å (*B*), 5823.5 Å (*C*); Figs. 2 (77 K) and 3 (4 K). In Fig. 2 the top spectrum was due to the sample under ultraviolet excitation. Two statements can be made:

(1) The spectra obtained in exciting directly into each of the *A*, *B*, *C* levels do not correspond to the fluorescence of an Eu^{3+} ion in a single site.

(2) For each excitation wavelength (λ_e) the same lines are observed but with very different relative intensities.

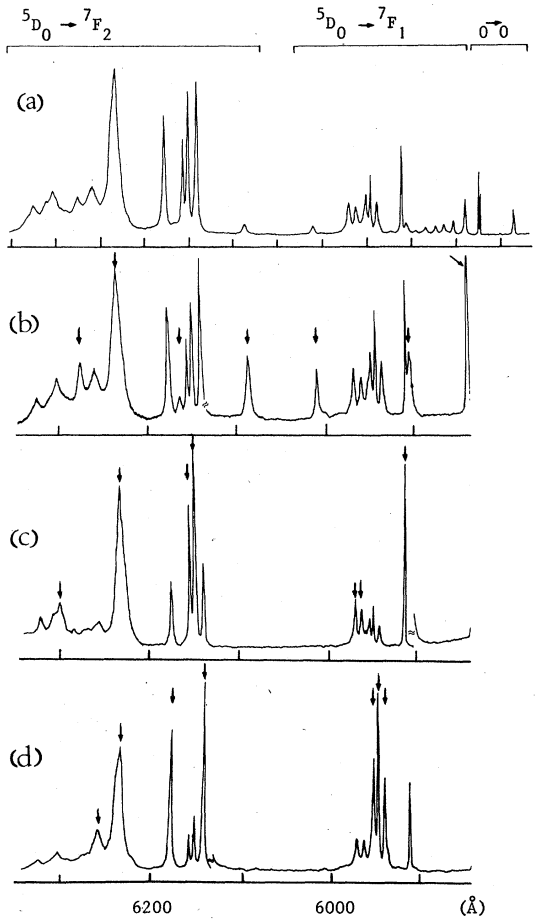

FIG. 2. Fluorescence of Eu^{3+} in monoclinic Gd_2O_3 at 77 K. (a): under uv excitation; (b): under laser excitation $\lambda_e = 5786$ Å (*A* spectrum); (c); under laser excitation $\lambda_e = 5822$ Å (*B* spectrum); (d): under laser excitation $\lambda_e = 5823.5$ Å (*C* spectrum). Arrows indicate lines from directly excited Eu^{3+} ions.

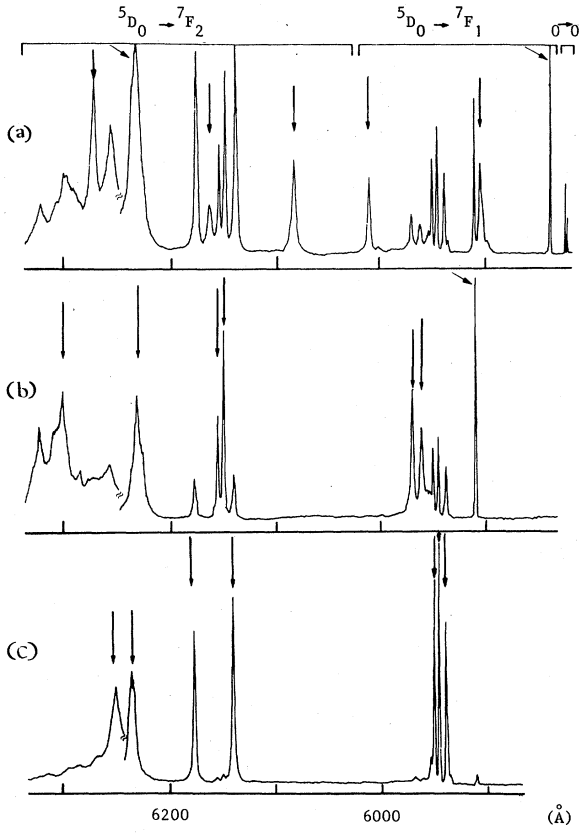

FIG. 3. Fluorescence of Eu^{3+} in monoclinic Gd_2O_3 at 4 K. (a): *A* spectrum; (b): *B* spectrum; (c) *C* spectrum.

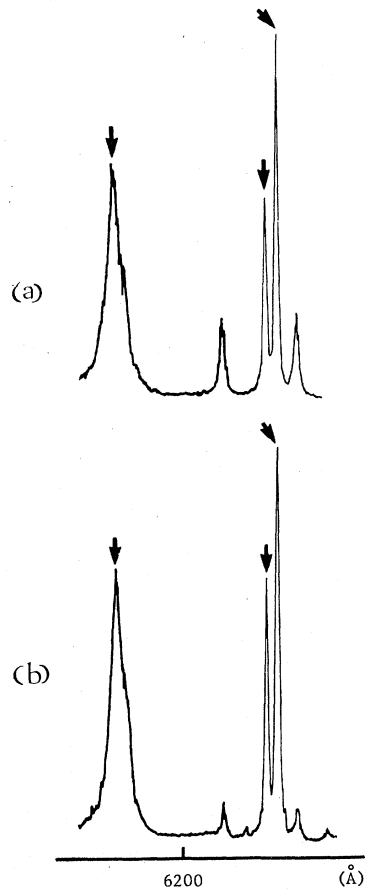

FIG. 4. Comparison of continuous selective excitation (a) and pulsed selective excitation (b) $\lambda_e = 5822$ Å; arrows indicate lines directly excited.

Two conclusions arise immediately:

(a) There is always energy transfer from site to site in this compound, so that fluorescence from a Eu^{3+} not directly excited appears after transfer; this problem will be considered later.

(b) Fluorescence lines arising from Eu^{3+} ions whose $^5D_0$ level is in exact resonance with the laser wavelength are always greatly enhanced with respect to the others.

Accordingly, we can separate $^5D_0 \rightarrow {}^7F_{0\text{-}4}$ emission into three groups of lines originating from distinct Eu^{3+} sites (Table I). In the present case it was possible to distinguish the spectra emitted by Eu^{3+} occupying distinct crystallographic sites even under continuous selective excitation. Only some ambiguities remain when several lines are in accidental coincidence. Some weak lines appearing on the long-wavelength side of the $^5D_0 \rightarrow {}^7F_2$ transition could not be attributed to any particular spectrum; these are probably vibronic components and are referred to as "*v*" in Table I.

B. Time-resolved fluorescence

As can be seen in Fig. 4 the selective excitation was improved when using a time-resolved method. The upper spectrum was measured for $\lambda_e(B)$ under continuous excitation, and the lower spectrum with a 35-μs delay between the excitation pulse and the detection, so that energy transfer from *B* to *C* was not completely accomplished and *B* lines were enhanced relative to *C* lines which were almost suppressed.

VI. ASSIGNMENT OF THE OBSERVED SPECTRA TO THE CRYSTALLOGRAPHIC SITES

The large differences observed between the three $^5D_0 \rightarrow {}^7F_1$ spectra in particular reveal large differences between second-order crystal-field parameters which must be highly structure dependent. The best way to assign each experimen-

TABLE I. Laser site selective excitation: numerical results ($T = 4$ K).

Transition	λ (Å)	E (cm^{-1})	ΔE (cm^{-1})	Barycenter	Identification after Ref. 1 Transition	Nature
A spectrum						
$^5D_0 \rightarrow {}^7F_0$	5786	17283			$^5D_0 \rightarrow {}^7F_0$	σ
$^5D_0 \rightarrow {}^7F_1$	5838	17129	154		$^5D_1 \rightarrow {}^7F_3$	π
	5904	16938	345	381	$^5D_1 \rightarrow {}^7F_3$	σ
	6010	16639	644			
$^5D_0 \rightarrow {}^7F_2$	6085(1)	16434	849		$^5D_2 \rightarrow {}^7F_6$	σ
	6165(2)	16221	1062		$^5D_0 \rightarrow {}^7F_2$	σ
	6235(3)	16038	1245	1070		
	6274(4)	15939	1344	[line(1):	$^5D_1 \rightarrow {}^7F_4$	σ
	6293(ψ)	15888	1395	doublet]		
	6310(ψ)	15848	1435			
$^5D_0 \rightarrow {}^7F_3$	6462	15475	1808			
	6485	15420	1863			
	6488	15413	1870			
	6537	15297	1986	2009		
	6597.5	15157	2126			
	6620	15106	2177			
	6644	15050	2233			
$^5D_0 \rightarrow {}^7F_4$	6880	14535	2748			
	6926	14438	2845			
	7065	14154	3129			
	7082	14120	3163			
	7084.5	14115	3168			
	7132	14021	3262			
	7140	14006	3277			
B spectrum						
$^5D_0 \rightarrow {}^7F_0$	5822	17176			$^5D_0 \rightarrow {}^7F_0$	σ
$^5D_0 \rightarrow {}^7F_1$	5910	16920	256		$^5D_1 \rightarrow {}^7F_3$	σ
	5961	16776	400	360	$^5D_0 \rightarrow {}^7F_1$	σ
	5969	16752	424		$^5D_0 \rightarrow {}^7F_1$	π
$^5D_0 \rightarrow {}^7F_2$	6150(1)	16260	916		$^5D_0 \rightarrow {}^7F_2$	σ
	6155.5(2)	16246	930		$^5D_0 \rightarrow {}^7F_2$	σ
	6232.5(3)	16045	1131	1040		
	6302.5(4)	15867	1309	[line (1):		
				doublet]		
	6325(ψ)	15810	1366			
$^5D_0 \rightarrow {}^7F_3$	6517.5	15343	1833			
	6535	15302	1874			
	6538.5	15294	1882			
	6558	15249	1927			
	6573.5	15212	1964			
	6613.5	15121	2055			
$^5D_0 \rightarrow {}^7F_4$	6873.5	14549	2627			
	6947	14395	2781			
	6957	14374	2802			
	6964	14360	2816			
	7025.5	14234	2942			
	7058	14168	3008			
	7059.5	14165	3011			
	7073.5	14137	3039			
	7096.5	14091	3085			

TABLE I. (*Continued*)

Transition	λ (Å)	E (cm^{-1})	ΔE (cm^{-1})	Barycenter	Identification after Ref. 1 Transition	Nature
C spectrum						
$^5D_0 \rightarrow {}^7F_0$	5823.5	17172			$^5D_0 \rightarrow {}^7F_0$	σ
$^5D_0 \rightarrow {}^7F_1$	5939	16838	334		$^5D_0 \rightarrow {}^7F_1$	π
	5945	16821	351	349	$^5D_0 \rightarrow {}^7F_1$	σ
	5949.5	16809	363		$^5D_0 \rightarrow {}^7F_1$	π
$^5D_0 \rightarrow {}^7F_2$	6140.5(1)	16285	887		$^5D_0 \rightarrow {}^7F_2$	σ
	6177.5(2)	16188	984		$^5D_0 \rightarrow {}^7F_2$	σ
	6235(3)	16038	1134	1007		
	6239(4)	16028	1144	[line (1): doublet]	$^5D_1 \rightarrow {}^7F_4$	π
	6257.5(υ)	15981	1191			
$^5D_0 \rightarrow {}^7F_3$	6519	15340	1832			
	6533	15307	1865			
	6543.5	15282	1890			
	6560	15244	1928			
	6567.5	15226	1946			
	6605	15140	2032			
$^5D_0 \rightarrow {}^7F_4$	6842	14616	2556			
	6941	14407	2765			
	6966	14353	2819			
	7000	14286	2886	2904		
	7020.5	14244	2928			
	7066	14152	3020			
	7073	14138	3034			
	7080	14124	3048			
	7094.5	14095	3077			

tal spectrum *A*, *B* and *C* to a particular C_s site I, II, III is the following:

Determination of three sets of *ab initio* calculated crystal-field parameters relative to Ln I, Ln II and Ln III, respectively.

Diagonalization of the crystal-field interaction matrix to obtain theoretical energy levels.

Comparison of each spectrum with calculated values.

A. *A priori* calculation of B_q^k

The crystal-field Hamiltonian associated with a C_s symmetry may be described by 14 b_q^k and s_q^k values ($B_q^k = b_q^k + is_q^k$). *Ab initio* B_q^k values were calculated following the electrostatic model (EM), utilizing the recent structure refinement of monoclinic Eu_2O_3 carried out by Yakel.[5] The author admits the possibility of a *Cm* or *C*2 space group instead of *C*2/*m* owing to an eventual slight displacement of ions from symmetry elements, but as it stands, the indices of agreement after the *C*2/*m* refinement are low enough to warrant precise positional parameters, which is an essential condition for *a priori* calculations.

Two contributions to the multipolar crystal-field development were taken into account: the point charge contribution (PC) and the induced dipoles contribution (ID). In a previous paper (Ref. 6), it was shown that the addition of dipolar effects improved the EM results in the particular cases of Nd_2O_3 and Nd_2O_2S. The mathematical details may be found in Ref. 6. The same method was applied to Eu^{3+} in the three crystallographic sites of Gd_2O_3. The results are summarized in Table II. Two corrections are made to the crude (PC + ID) values:

(a) A shielding parameter correction (PC + ID) $(1 - \sigma_k)$ which measures the reduction of the $B_q^k C_q^k$ term of the crystal-field expansion at the 4*f* site, due to the shielding effect of 5*s* and 5*p* electrons. Gupta and Sen[7] calculated a σ_2 value of 0.686 for Eu^{3+}. σ_4 and σ_6 were set equal to 0.139 and 0.109, respectively [values for Nd^{3+} (Ref. 6)]

(b) An "expansion" correction to obtain "lattice" radial integrals from free-ion radial integrals. A similar line of argument was followed by Karayianis and Morrison[8] who stated that the Har-

TABLE II. Calculated $B_q^k(\mathrm{cm}^{-1})$. $B_q^k = b_q^k + i\, s_q^k$ reference axes: z parallel to b (crystallographic axis), y rotated of β around z from c (crystallographic axis) and x normal to z and y. (a) Point charge contribution (PC). (b) Induced dipole contribution (ID). (c) Total contribution (PC+ID). (d) Corrected total contribution $(\mathrm{PC}+\mathrm{ID})(1-\sigma_k)\, c_k$ (see text).

	Ln I $\beta=-43°$				Ln II $\beta=-31°$				Ln III $\beta=-41°$			
	(a)	(b)	(c)	(d)	(a)	(b)	(c)	(d)	(a)	(b)	(c)	(d)
b_0^2	0	573	573	252	361	133	494	217	238	292	530	233
b_2^2	151	143	294	129	−699	−70	−769	−338	1744	241	1985	873
s_2^2	200	−200	0	0	−588	588	0	0	−305	305	0	0
b_0^4	−175	11	−164	−279	−183	−28	−211	−359	−120	80	−40	−68
b_2^4	382	142	524	891	−678	55	−623	−1059	−743	−86	−829	−1409
s_2^4	−680	45	−635	−1079	−353	26	−327	−556	−797	−64	−861	−1464
b_4^4	322	−30	292	496	−211	−8	−219	−372	288	8	296	503
s_4^4	−153	−13	−166	−282	−317	30	−287	−488	355	96	451	767
b_0^6	−200	−11	−211	−485	−216	10	−206	−474	−226	−34	−260	−598
b_2^6	48	26	74	170	−37	−5	−42	−97	40	−1	39	90
s_2^6	−5	−7	−12	−28	−40	8	−32	−74	−57	−9	−68	−156
b_4^6	−52	11	−41	−94	55	−16	39	90	−96	3	−93	−214
s_4^6	−12	−11	−23	−53	93	−24	69	159	51	−10	41	94
b_6^6	−2	−1	−3	−7	32	17	49	113	45	−18	27	62
s_6^6	100	−19	81	186	−9	9	0	0	83	17	100	230

tree-Fock wave functions were inadequate even for reproducing free-ion empirical Slater integrals. Free and bound states radial functions should have similar expansions but far stronger than those exhibited by the theoretical Hartree-Fock functions. To take this into account, they introduced an additional parameter τ in the wave function, with the effect of replacing $\langle r^k \rangle$ by $\tau^{-k}\langle r^k \rangle$. τ was fitted by comparison from the experience.

Ours was a different procedure which was already applied in Ref. 6. The experimental F^2, F^4 and F^6 from Ref. 9 were compared to the theoretical (Hartree-Fock) F^k, and their lowering allowed for a crude estimation of true $\langle r^k \rangle$. In the present case, F^2, F^4, and F^6 were unknown, so we adopted the same corrections as in Ref. 6, i.e., we supposed that the radial wave functions of Eu^{3+} were expanded in the same way as Nd^{3+}, so that $\langle r^2 \rangle$, $\langle r^4 \rangle$, and $\langle r^6 \rangle$ (from Freeman and Watson[10]) were multiplied by $c_k = 1.4$, 2, and 2.6, respectively, in the Gd_2O_3 matrix.

The lack of accurate polarizability values is probably the crucial point. We set $\alpha(O^{2-}) = 2\,\text{Å}^3$, $\alpha(Eu^{3+}) \simeq \alpha(Nd^{3+}) = 1\,\text{Å}^3$.

The final results $(\mathrm{PC}+\mathrm{ID})(1-\sigma_k)c_k$ are reported in Table II.

B. Calculated spectra: Assignment

Ab initio B_q^k are introduced in the order 49 complex interaction matrix, including spin-orbit coupling and crystal-field interactions, within the $^7F_{J,M}$ sublevels (Ref. 11). In the theoretical spectra I, II, and III, the overall splittings of the $^7F_1$ level are equal to 114, 153, and 398 cm^{-1}, respectively. These values are to be compared with the experimental values (Table I), i.e., 490, 168, and 29 cm^{-1} for A, B, and C, respectively.

Though there is no rigorous one-to-one coincidence between the calculated and experimental sets, it is inviting to identify site III with spectrum A, site II with spectrum B, and site I with spectrum C (a larger discrepancy occurs in the last correlation). This assumption is reinforced by the inspection of the whole energy scheme of the $^7F_J (J = 1$ to 4) manifold as compared with III, II, I, respectively (Fig. 5). One can see that the agreement is fairly good.

In the previous work by Rice and de Shazer[1] (on

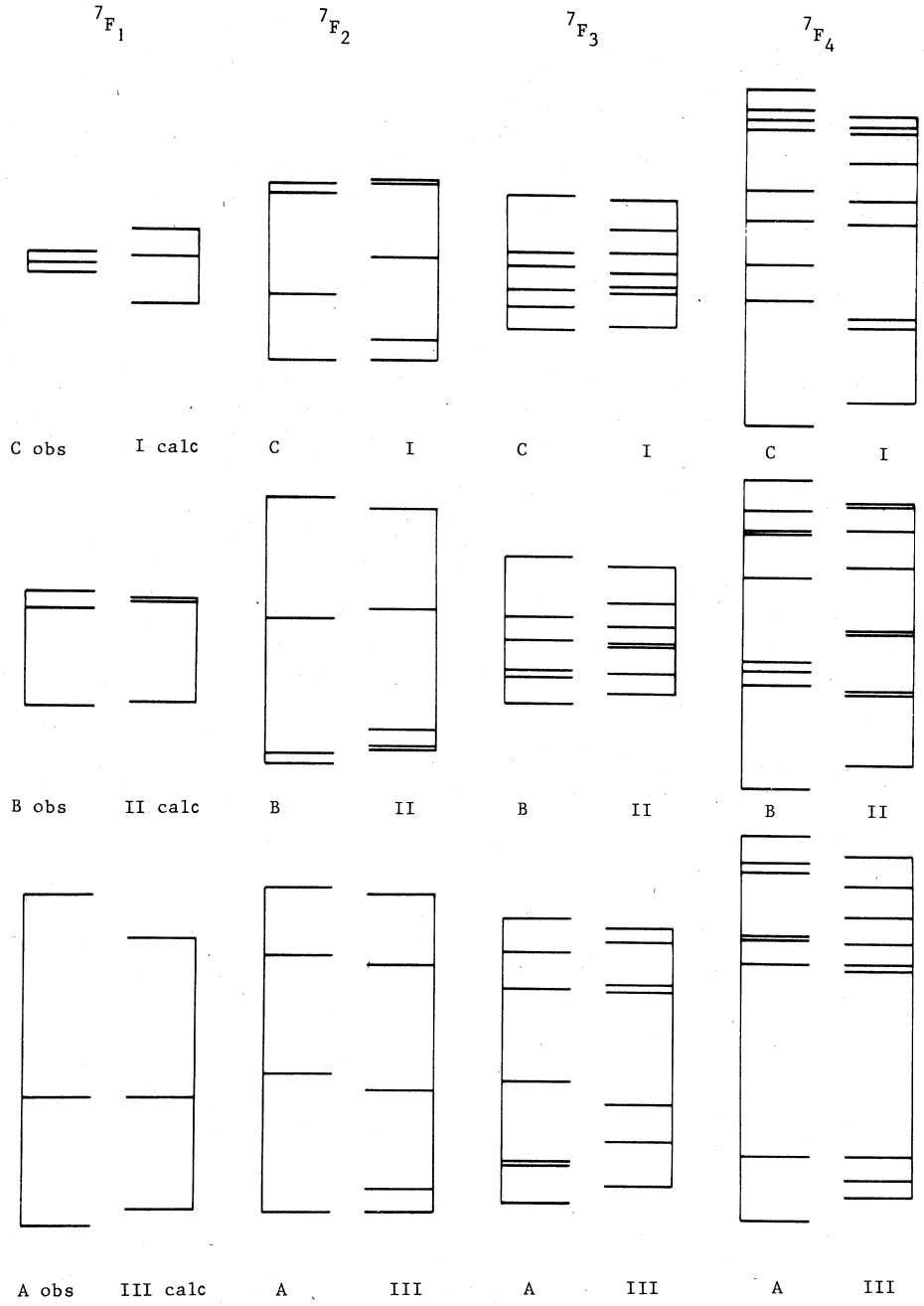

FIG. 5. Comparison of observed and calculated level positions.

a single crystal presumably untwinned), polarization measurements were performed in order to identify the irreducible representations associated with each sublevel, but important discrepancies arise by comparison with our own results. Concerning, for example, $^5D_0 \rightarrow {}^7F_1$ (see Table I), their identification leads to $(2\sigma + \pi)$ lines for spectrum B and $(2\pi + \sigma)$ for spectrum C, results which are unconsistent. In a C_s symmetry, the $J = 1$ representation is reduced to $(A' + 2A'')$ which should lead to $(\sigma + 2\pi)$ in both cases. In fact, the authors mention the lack of precision of the polarization measurements of fluorescent transitions which is probably responsible for these discrepancies.

Consequently we cannot utilize their results, and since the symmetry labels of experimental levels are unknown, it seems meaningless to attempt any refinement of crystal-field parameters.

Three other diagonalizations were performed with point-charge contributions only in B_q^k values (with the same shielding and radial integral corrections). The overall splittings of the $^7F_1$ sublevels are then equal to 53, 175, and 364 cm^{-1} for I, II, and III, respectively. Surprisingly enough, the agreement is better than with dipolar corrected parameters. Owing to the weak influence of dipolar corrections to B_q^4 and B_q^6, the aspect of the remaining levels $^7F_2$, $^7F_3$ and $^7F_4$ is not much changed. Once more, the lack of symmetry information makes it impossible to decide whether the use of the correction is, on a whole, beneficial or not, in this particular case. Three points need to be emphasized:

(a) Second-order parameters are very sensitive to small atomic displacements. When structural information from the earlier work of Hubbert-Paletta and Muller-Buschbaum[4] is utilized, even larger B_q^2 values are found for Ln I. It is evident that the new structure (Ref. 5) works better.

(b) Sengupta and Artman[12] found, for Nd^{3+}-and Np^{4+}-doped $PbMoO_4$, a dipolar contribution equal to ten times the monopolar contribution. They then expressed some doubt concerning "the validity of the convergence of a multipolar lattice-sum analysis". It is true that our dipolar corrections are not so large, but it is obvious that a quadrupolar calculation would help to clear up the matter.

(c) In a recent paper, Newman[13] emphasized the correlation between the nephelauxetic series and ligand polarizability. As pointed out by this author, crystal-dependent O^{2-} polarizability should then be reflected by variation of Slater shifts. In the present case, there exists a quite important nephelauxetic shift between B and C spectra on the one hand ($^5D_0 \rightarrow {}^7F_0 \sim 5820$ Å) and the A spectrum on the other hand ($^5D_0 \rightarrow {}^7F_0 \sim 5790$ Å); $\Delta \simeq 100\ cm^{-1}$. However, the Eu^{3+} case is complex and it was shown[14] that the raising of the $^5D_0$ level in solids cannot be related to an unambiguous variation of F^2, F^4, and F^6, but *only* to a preferential decrease of F^2 with respect to F^4 and F^6. Besides, in the present case, we should rather speak about a "site-dependent" O^{2-} polarizability since this ion occupies five different crystallographic sites in

TABLE III. Contribution from first neighbors to calculated (B_q^2) ID. R, θ, φ are the polar coordinates of a ligand and M_x, M_y the Cartesian coordinates of induced dipoles at the ligand site.

	Ligand	M_x (eÅ)	M_y (eÅ)	R (Å)	θ (°)	φ (°)	$(B_0^2)d$ (cm^{-1})	$(b_2^2)d$ (cm^{-1})
	0(1)(2)	0.319	−0.059	2.537	135.2 44.8	−125.7	−144	162
	0(3)(2)	0.157	0.160	2.290	141.9 38.1	14	364	35
Ln I	0(3)	−0.157	−0.160	2.656	90	−65.6	−66	52
	0(4)	0.153	0.057	2.413	90	168.5	165	−154
	0(4)	−0.153	−0.057	2.298	90	97.6	53	13
	Total first neighbors Ln I						592	305
	0(1)(2)	0.324	0.011	2.462	137 43	99.5	−53	68
	0(2)(2)	−0.016	−0.010	2.297	141.6 38.4	−118.8	32	−5
Ln II	0(1)	0.016	0.010	2.288	90	−55.6	0	−21
	0(3)	−0.119	−0.1905	2.340	90	30.2	268	−263
	0(5)	0	0	2.739	90	175.1	0	0
	Total first neighbors Ln II						226	−158
	0(4)(2)	0.1509	0.062	2.254	143. 37.	54.4	285	−60
	0(5)(2)	0	0	2.544	135.1 44.9	−106.4	0	0
Ln III	0(1)	0.320	−0.049	2.308	90	−19.9	−454	380
	0(2)	0.017	0.007	2.239	90	177.1	28	−32
	0(3)	−0.153	−0.165	3.132	90	107.6	47	8
	Total first neighbors Ln III						191	236

monoclinic Gd_2O_3.

Table III reports the first-neighbor contribution to the dipolar correction of the B_q^2 for I, II, and III sites. Note that convergence is far from effective at the first coordination shell. In fact the convergence of $(B_q^2)_{ID}$ behaves like $\sum_i f(i)/R^4$. It is intermediate between the convergence of $(B_q^2)_{PC}$ and $(B_q^4)_{PC}$ so that sufficiently accurate values are obtained by a summation within a 8-Å radius sphere. However the largest discrepancy between calculated and experimental B_q^2 occurs for Ln I and precisely in this case are the contributions of farther neighbors quite small (at least for B_0^2). Table III underlines that the high (undesirable) B_0^2 value originates from a very high O(3) positive contribution which competes with a negative O(1) contribution. Changes in O^{2-} polarizability values from site to site should modify their relative magnitudes, but further discussion of the matter at this stage can only be highly speculative.

VII. ENERGY TRANSFERS

In this section we would like to point out some characteristics of fluorescence transient properties without attempting any theoretical treatment of energy transfer from site to site. In such a multisite compound doped with europium and in our experimental conditions, the only way for energy to transfer from a donor site D (equivalent to sensitizer ion) to an acceptor site A (equivalent to activator ion) is by a process:

$$Eu^{3+}D(^5D_0) + Eu^{3+}A(^7F_0) \rightarrow Eu^{3+}D(^7F_0) + Eu^{3+}A(^5D_0)$$

As was already mentioned, we always observe energy transfer from site to site in Gd_2O_3 even at low temperatures. As can be seen from Figs. 2 and 3, transfer takes place at 77 K either towards lower or higher energies: $A \rightleftharpoons B \rightleftharpoons C$. At 4 K the $B \rightarrow A$ transfer is completely inhibited but $C \rightarrow B$ appears very weakly, the 4-cm^{-1} energy difference between the two corresponding $^5D_0 \rightarrow {}^7F_0$ transitions being of the same order as kT. In Fig. 6 are shown the fluorescence rise and decay times of of $^5D_0$ levels. Two kinds of experiment were performed at 4 K:

First, excitation of $^7F_0 \rightarrow {}^5D_0$ (A, B, or C site) and measurement of $^5D_0 \rightarrow {}^7F_{1,2}$ (A, B, or C site) respectively. In these conditions the fluorescence rise is too fast to be followed by the apparatus.

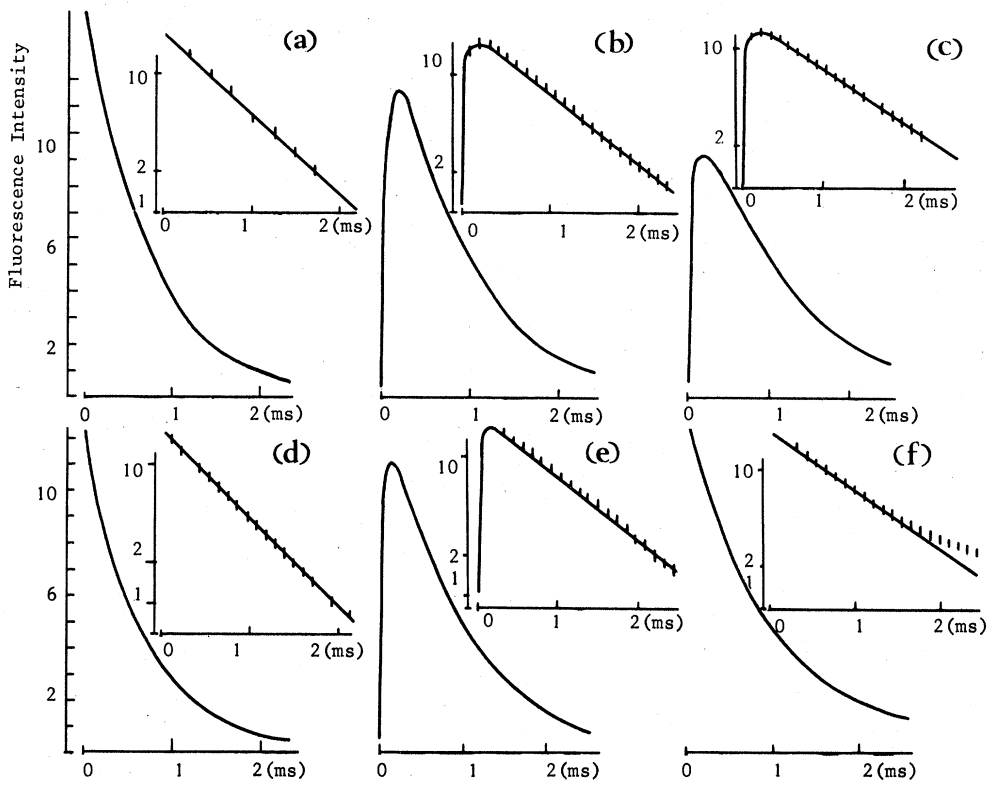

FIG. 6. Fluorescence rise and decay times measurements at 4 K. (a): excitation (exc.) C (λ_e=5823.5 Å), analysis (anal.) C (λ_a=6140 Å); (b): exc. B (λ_e=5822 Å), anal. C; (c): exc. A (λ_e=5786 Å), anal. C; (d): exc. B, anal. B (λ_a=6150 Å); (e): exc. A, anal. B; (f): exc. A, anal. A (λ_a=6085 Å).

The decays of B and C ($^5D_0$) levels are exponential $\tau(C)=0.72$ ms is the real radiative lifetime (neglecting back-transfer $C \rightarrow B$); $\tau(B)_{\text{apparent}}=0.68$ ms is the apparent radiative lifetime of Eu^{3+} in B (donor) sites in presence of Eu^{3+} in C (acceptor) sites. The $A(^5D_0)$ level decay is more complex due to multiple transfers from this more energetic level, and does not exactly follow an exponential law, nevertheless we can estimate the apparent radiative lifetime $\tau(A)_{ap}$ to be longer than $\tau(B)_{ap}$ and $\tau(C)$.

Second, excitation of $^7F_0 \rightarrow {}^5D_0$ donor site (A or B) and measurement of $^5D_0 \rightarrow {}^7F_{1,2}$ acceptor site (B or C): see Figs. 6(b), 6(c), and 6(e). In these cases the fluorescence rise time is much larger due to donor → acceptor energy transfer. The rate equations describing, for example the B (donor) → C (acceptor) system are

$$\begin{aligned}\frac{dN_B^*}{dt} &= N_B(t)\Phi(t)\sigma - W_B N_B^*(t) - W_{BC} N_B^*(t)N_C(t) \\ &\quad + W_{CB} N_C^*(t)N_B(t), \\ \frac{dN_C^*}{dt} &= W_{BC} N_B^*(t)N_C(t) - W_{CB} N_C^*(t)N_B(t) - W_C N_C^*(t),\end{aligned} \tag{1}$$

where $N_B(t)$ and $N_C(t)$ are the $^7F_0$ level populations in B and C sites. These values are generally assumed to be constants due to low power excitation. In this particular case $N_B(t)=N_C(t)=N$ because the substitution Eu^{3+}/Gd^{3+} is equal on the three sites. $N_B^*(t)$ and $N_C^*(t)$ are the excited $^5D_0$ level populations for B and C, respectively. W_{BC} and W_{CB} are the transfer probabilities from B to C and C to B and are supposedly time independent. $W_C=1/\tau(C)$ and W_B are the radiative lifetimes of Eu^{3+} $^5D_0$ in C and B sites. $\Phi(t)$ is the excitation flux and σ is a constant proportional to the oscillator strength of the absorbing transition. To simplify the resolution of these equations we have assumed the following conditions: that the initial populations are $N_B^*(0)=N_0^*$ and $N_C^*(0)=0$ at the end of the pulse, and that there is no back transfer ($W_{CB}=0$). The simplified rate equations are then

$$\begin{aligned} dN_B^*/dt &= -W_B N_B^*(t) - W_{BC} N N_B^*(t), \\ dN_C^*/dt &= +W_{BC} N N_B^*(t) - W_C N_C^*(t). \end{aligned} \tag{2}$$

Equations (1) were applied by several authors to materials in which active Ln^{3+} ions are either a constituent (PrF_3, $PrCl_3$, Ref. 15), or a dopant ($CaWO_4$:Eu^{3+}, Sm^{3+}, Ref. 16). The integration of Eqs. (2) leads to $N_B^*(t)=N_0^* \exp[-(W_B+W_{BC}N)t]$. The value $(W_B+W_{BC}N)$ is extracted from the B decay curve as being $1/\tau(B)_{ap}$.; $N_C^*(t) = W_{BC}N_0^*N[\exp(-W_C t)-\exp(-W_B-W_{BC}N)t]/W_B+W_{BC}N-W_C$. However because $(W_B+W_{BC}N) = 1/\tau(B)_{ap} \simeq W_C = 1/\tau(C)$ in this particular case, with the approximations $W_B+W_{BC}N=W_C+\epsilon$ and $e^{-\epsilon t} \sim 1-\epsilon t$ we obtain in fact $N_C^*(t) = W_{BC}N_0^*N[t\exp(-W_C t)]$. $N_C^*(t)$ is then maximum for $t_M=1/W_C=\tau(C)=720$ μs and the theoretical decay time of C after transfer from B is found to be $\tau(C)_{BC}=1.4$ ms. These results are obviously in contradiction with experimental data [$t_M=250$ μs, $\tau(C)_{BC}=0.790$ ms]. The model employed is thus oversimplified probably mainly by neglecting back-transfer $C \rightarrow B$, and by assuming $N_C^*(0)=0$ which is not true taking into account the pulse duration (30 μs).

VIII. DISCUSSION

The accuracy of the one-to-one correspondence between experimental site-selected fluorescence spectra of Eu^{3+}-doped monoclinic Gd_2O_3 on one hand and crystallographic europium sites on the other hand entirely depends on the reliability of the electrostatic model for *a priori* calculations of crystal-field parameters. The good analogy between calculated and experimental spectra gives us some ground to believe that our conclusions are valid.

The assumption that the expansion of the radial wave functions of the lanthanide ion in the crystalline matrix is the main source of discrepancy between calculated and experimental B_q^k was discussed earlier by Karayianis and Morrison[8] and Devine and Berthier[17]. The latter compared, for ten different rare-earth compounds (insulator or weakly metallic), effective $\langle r^k \rangle$ ($k=4$ and 6) derived from experimental spectra, with new theoretical values calculated by Freeman and Desclaux[18] (FD) for trivalent rare-earth ions. They noted an increasing discrepancy (experimental $\langle r^4 \rangle$/calculated $\langle r^4 \rangle$) with increasing atomic number, whatever the type of bonding.

We may compare the results of the present work (Eu^{3+} in Gd_2O_3) together with earlier results[19] (Eu^{3+} in $LaAlO_3$) with those obtained in Ref. 6 (Nd^{3+} in Nd_2O_3 and Nd_2O_2S). For Nd^{3+}, the effective $\langle r^4 \rangle$ is about equal to 3.3 a.u., that is, 1.14 times the (FD) theoretical value. For Eu^{3+}, the effective $\langle r^4 \rangle$ is 3.06 a.u., that is, 1.5 times the (FD) free-ion value. This supports Devine's[17] statement as far as the variation of discrepancy of $\langle r^4 \rangle$ with the atomic weight is concerned. Considering a quite different compound[20], europium-doped KY_3F_{10}, the effective $\langle r^4 \rangle$ is equal to about 1.4 times the (FD) theoretical value, and this ratio is not very far from that of Eu^{3+} in oxides (see above). This seems consistent with the second part of Devine's statement, that is, the nonsensitivity of $\langle r^4 \rangle$ to the nature of the bonding.

However, a counter example to the proposed

hypothesis can be found in a recent paper of Morrison and Leavitt[21], concerning crystal-field analysis of rare-earth doped trifluorides. Following this work, the apparent $\langle r^4 \rangle$ of Eu^{3+}, for example, is equal to 6.16 a.u. The lattice sum analysis was based on a recent neutron diffraction structure refinement, and the crystal-field analysis on the true C_2 site symmetry. Indeed, calculated values are very sensitive to the way lattice sums are carried out. For instance, results quoted by Devine and Berthier[17] concerning $Y_3Al_5O_{12}$;Ln^{3+} and $CaWO_4$:Ln^{3+} were derived[8,22] by lattice sums on *nonionic* charges ($q_{Al} = 1.92e$, $q_O = -1.55e$ in the former case for instance). The aim of this remark is only to stress the difficulty of comparing different sets of results in a fully consistent way.

Yet, it remains true that in similar sorts of compounds such as mixed oxides actually under consideration, the effective $\langle r^k \rangle$ of a given trivalent rare earth display nearly identical values. We have already made this statement for Eu^{3+} in $LaAlO_3$ (Ref. 19), Y_2O_3 (Ref. 11), Nd_2O_3 (Ref. 6), and Gd_2O_3 (this work).

Although some details remain unsolved, the agreement between observed and calculated level positions as schematized on Figure 5 seems to us quite satisfactory. We think that this work gives proof of the actual usefulness of the electrostatic model, especially when applied to compounds exhibiting several different low-symmetry crystallographic sites for the rare earth.

ACKNOWLEDGMENT

The authors wish to thank Dr. F. Auzel (Centre National d'Etude des Telecommunications Bagneux, France) for useful discussions concerning energy transfers.

[1]D. K. Rice and L. G. de Shazer, J. Chem. Phys. 52, 172 (1970).
[2]O. Beaury, J. Dexpert-Ghys, M. Faucher, and P. Caro, J. Lumin. 18/19, 249 (1979).
[3]D. T. Cromer, J. Phys. Chem. 61, 753 (1957).
[4]E. Hubbert-Paletta and H. Muller-Buschbaum, Z. Anor. Allg. Chem. 363, 3 (1968).
[5]H. L. Yakel, Acta Cryst. B35, 564 (1979).
[6]M. Faucher, J. Dexpert-Ghys, and P. Caro, Phys. Rev. B 21, 3689 (1980).
[7]R. P. Gupta and S. K. Sen, Phys. Rev. A 7, 850 (1973).
[8]N. Karayianis and C. A. Morrison, U. S. National Technichal Report Information Service, Springfield, Va., Report No. A011252.
[9]P. Caro, J. Derouet, L. Beaury and E. Soulie, J. Chem. Phys. 70, 2542 (1979).
[10]A. J. Freeman and R. E. Watson, Phys. Rev. 127, 2058 (1962).
[11]J. Dexpert-Ghys and M. Faucher, Phys. Rev. B 20, 10 (1979).
[12]D. Sengupta and J. O. Artman, Phys. Rev. B 1, 2986 (1970).
[13]D. J. Newman, Aust. J. Phys. 30, 315 (1977).
[14]P. Caro, O. Beaury, and E. Antic, J. Phys. 37, 671 (1976).
[15]D. S. Hamilton, P. M. Selzer, and W. M. Yen, Phys. Rev. B 16, 1858 (1977).
[16]R. G. Peterson and R. C. Powell, J. Lumin. 16, 285 (1976).
[17]R. A. B. Devine and Y. Berthier, Solid State Commun. 26, 315 (1978).
[18]A. J. Freeman and J. P. Desclaux, J. Magn. Magn. Mater. 12, 11 (1979).
[19]M. Faucher and P. Caro, J. Chem. Phys. 63, 446 (1975).
[20]P. Porcher and P. Caro, J. Chem. Phys. 65, 89 (1976).
[21]C. A. Morrison and R. P. Leavitt, J. Chem. Phys. 71, 2366 (1979).
[22]C. A. Morrison, D. E. Wortman, and N. Karayianis, J. Phys. C 9, L191 (1976).